PERGAMON

International Journal of Heat and Mass Transfer 43 (2000) 1121–1131

International Journal of HEAT and MASS TRANSFER

www.elsevier.com/locate/ijhmt

Coupling of conduction and convection past an impulsively started semi-infinite flat plate

Amilcare Pozzi*, Renato Tognaccini

Dipartimento di Progettazione Aeronautica, Universita' di Napoli 'Federico II', Piazzale V. Tecchio 80, 80125 Naples, Italy

Received 8 February 1999; received in revised form 10 June 1999

Abstract

A quasi-analytical solution of the conjugated heat transfer problem for a semi-infinite flat plate that is impulsively accelerated in a compressible laminar flow with Prandtl number equal to 1 is proposed. The solution is based on an integral formulation both for the momentum and energy equations in the fluid and for the thermal coupling between the fluid and the solid. The results are compared to previously obtained exact solutions in the limiting conditions of 'asymptotic' and 'steady' flow. The influence on the temperature field of the main parameters characterizing the problem is discussed.

1. Introduction

The subject of the present work is the analysis of the velocity and temperature field when a semi-infinite thick and thermally conductive flat plate is impulsively accelerated in a fluid at rest wetting one side of the plate and a given temperature is suddenly imposed on the other side. The solution of the energy equation in an unsteady flow around a body at high speeds is further complicated if, as in practical cases, neither the temperature nor the heat flux are known at the solid–fluid interface. This problem, called the conjugated heat transfer, assumes as boundary condition at the interface the continuity of the temperature and of the heat transfer. Its solution is still difficult even if the assumption of a laminar boundary layer is made because of the spatial nature of the energy equation in the solid remains of elliptic type. In fact, only few results are available in the literature and essentially in steady regimes. Luikov et al. [1] presented an analytical but complex solution without numerical results. The problem was simplified in the case of elongated bodies by using an expansion in series of the ratio between normal and axial characteristic lengths of the body, thus obtaining that the temperature is proportional to the heat flux at the interface. Mori et al. [2,3] investigated, using the eigen functions technique, the effect on the Nusselt number of the boundary conditions (constant temperature or constant heat flux) at the outer wall. Pozzi, Bassano and de Socio [4] found the solution for the impulsive flow around a flat plate of infinite length by solving a problem with two independent variables, t (time) and y (coordinate normal to the plate). In the present work a flat plate of semi-infinite length is considered together with a fluid characterized by a Prandtl number of one. The boundary conditions at the solid–fluid interface are similar to those used for the infinite plate and are obtained by neglecting the axial conduction in the solid [4]. A low accurate simple solution of the same problem was proposed in [5] considers only the coupling condition without satisfying the energy equation.

In the case of semi-infinite flat plate there are three

* Corresponding author. Tel.: +39-08-17682185; fax: +39-08-17682187.

E-mail address: pozzi@unina.it (A. Pozzi).

0017-9310/00/$ - see front matter
PII: S0017-9310(99)00210-0

Nomenclature

b	plate thickness
d_0, d_1, A	constant values
g_i	coefficients of the Taylor expansion of u^+
H	$=h^2$
H_{tot}	total enthalpy
H_∞	free-stream total enthalpy
$h(X,\tau)$	scale factor of the dynamic boundary layer
J_{qw}	heat flux at solid–fluid interface
L	plate length
M_∞	free-stream Mach number
p	$=\frac{b}{L}\frac{\lambda_\infty}{\lambda_s}\sqrt{Re_\infty}$
Pr	Prandtl number
q_e	non-dimensional temperature imposed on the plate
q_i	coefficients of the Taylor expansion of S^+
Re_∞	Reynolds number
S	total enthalpy referenced to the free stream value
S^+	non-dimensional total enthalpy
T	temperature
T_e	temperature imposed on the plate
T_{aw}	adiabatic wall temperature in the case of steady flow and $b = 0$
T^+	non-dimensional temperature (referenced to T_∞)
t	time
t_{fs}	ratio between characteristic times of the fluid and solid
U_∞	free-stream velocity
U_n	Heaviside step function
u, v	velocity components
u^+	non-dimensional velocity component u
V	Stewartson–Dorodnitsin transformation of normal velocity component v
X	non-dimensional spatial coordinate x
x, y	spatial coordinates
Z	$=\mathrm{erf}(z)$
z	non-dimensional scaled spatial coordinate y

Greek symbols

α	thermal diffusivity
γ	ratio of the specific heats of the fluid
γ_1	$=2/\sqrt{\pi}$
δ	$=3t_{fs}p^2$
ζ	$=\frac{y\sqrt{Re_\infty}}{Lh}\eta$ Stewartson–Dorodnitsin transformation of spatial coordinate y
λ	thermal conductivity
μ	dynamic viscosity of the fluid
ν	cinematic viscosity of the fluid
ξ	non-dimensional independent variable of the energy equation in the steady region
τ	non-dimensional time

Subscripts

f	fluid property
ref	reference condition
s	solid property
x, y, t, X, Z, η, τ	specify partial derivation respect to the corresponding variable
w	solid–fluid interface condition
Z,0	partial derivative with respect to Z evaluated at $Z = 0$

independent variables: t, y and x (the coordinate in the plate direction). The temperature can be decoupled from the velocity field by the Stewartson–Dorodnitsin transformation. However, the phenomenon is still complex due to the presence of the leading edge of the plate. Three main regions for the temperature field have been found. In the first one (initial region) the influence of the leading edge is prevailing; 'very far' from the leading edge (asymptotic region), the solution tends to that presented in [4]; these regions are separated by a transition zone.

The solution has been obtained by applying an integral formulation of the boundary layer equations that reduces the number of independent variables by eliminating y. This procedure has already given good results in the case of steady flow on a flat plate with zero thickness with transport coefficients either constant or variable as shown in [6,7]. Preliminary results for the present case have been proposed in [8].

The first-order hyperbolic equation governing the problem has been solved in analytical form by the Lagrange's method. It highlights the physics of the phenomenon showing the regions that characterize the problem. The accuracy has been verified by comparing present results to the 'exact' solutions (in the sense that the 2D boundary layer equations are solved): unsteady infinite plate [4] and semi-infinite plate in steady flow [9].

In the following, after the description of the physical problem and solution method, the results will be dis-

cussed by analysing the behaviour of quantities of particular interest, such as the temperature and the heat flux at the solid–fluid interface. Moreover the effect of the main parameters characterizing the phenomenon (ratio between conductivities of the fluid and of the solid, Reynolds and Mach numbers, ratio between plate thickness and length) will be shown.

2. The physical and the mathematical problem

The geometry of the flow is sketched in Fig. 1. The semi-infinite, two-dimensional flat plate whose thickness is b, at the initial time $t = 0$ is impulsively accelerated to a constant speed U_∞ in a fluid with unit Prandtl number (Pr). The initial temperature field is uniform in both the fluid and the solid and is $T(x,y,0^-) = T_\infty$ where the subscript ∞ denotes free-stream conditions. For $t > 0$ a constant temperature T_e is impulsively imposed on the unwetted plate side.

We consider here a compressible laminar boundary layer arising near the plate. The flow equations can be simplified by adopting the Stewartson–Dorodnitsin transformation:

$$\eta = \int_0^y \frac{\rho}{\rho_\infty} \mathrm{d}y, \qquad V = \frac{\rho}{\rho_\infty} v + \eta_t + u\eta_x, \tag{1}$$

with u and v the velocity components. This transformation allows the continuity and momentum equation to be decoupled from the energy equation in the hypothesis $\frac{\rho}{\rho_\infty} = \frac{\mu_\infty}{\mu} = \frac{\lambda_\infty}{\lambda} = \frac{T_\infty}{T}$, where ρ, μ, λ are respectively the density, viscosity and conductivity of the fluid. With these assumptions the flow equations have the form

$$u_x + V_\eta = 0;$$

$$u_t + uu_x + Vu_\eta = \nu_\infty u_{\eta\eta};$$

$$S_t + uS_x + VS_\eta = \alpha_\infty S_{\eta\eta}; \tag{2}$$

where $S = H_{\mathrm{tot}} - H_\infty$ is the total enthalpy referenced to the free stream value and ν_∞, α_∞ denote the diffusivities in the fluid. Moreover, the energy equation in the solid is

$$T_{s,t} = \alpha_s\left(T_{s,xx} + T_{s,yy}\right), \tag{3}$$

where T_s is the temperature in the solid and α_s its diffusivity.

The boundary conditions we associate with Eqs. (2) and (3) are:

- (a) boundary conditions for the fluid field,

$$u\left(x,\infty,t^+\right) = U_\infty;\ S(x,\infty,t) = 0;$$

$$u(x,0,t) = V(x,0,t) = 0;$$

$$u(x,y,0^-) = 0;\ T(x,y,0) = T_\infty; \tag{4}$$

- (b) boundary conditions for the solid field,

$$T(x,y,0^-) = T_\infty, \tag{5a}$$

$$T\left(x,-b,t^+\right) = T_e; \tag{5b}$$

- (c) thermal boundary conditions at the solid–fluid interface,

$$T_s(x,0,t) = T_f(x,0,t);$$

$$\lambda_s T_{s,y}(x,0,t) = \lambda_f T_{f,y}(x,0,t); \tag{6}$$

where subscripts s and f denote respectively solid and fluid properties.

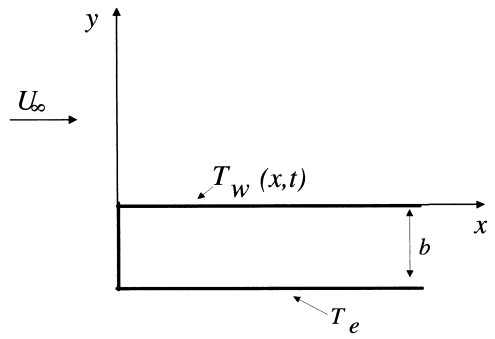

Fig. 1. The geometry of the problem.

3. The solution method

The solution method [7] reduces from three to two the number of the independent variables by integration of the Eq. (2), with respect to y, between 0 and ∞ and uses the Taylor formula in terms of a new variable $Z(\eta)$. With a suitable approximated expression of the remainder, the Taylor formula gives:

$$u^+(X,Z,\tau) = Z^n + \sum_{i=1}^{n-1} g_i(X,\tau)(Z^i - Z^n), \tag{7a}$$

$$S^+(X,Z,\tau) = \sum_{i=0}^{n-1} q_i(X,\tau)(Z^i - Z^n), \tag{7b}$$

where $u^+ = \frac{u}{U_\infty}$, $S^+ = \frac{S}{H_\infty}$, $Z(z) = \mathrm{erf}(z)$, (erf denotes the error function), $z = \frac{\eta\sqrt{Re_\infty}}{Lh(X,\tau)}$, $X = \frac{x}{L}$, $\tau = \frac{tL}{U_\infty}$, L is a reference length and

$$g_i(X,\tau) = \frac{1}{i!}\frac{\partial u^+}{\partial Z^i}(X,0,\tau),$$

$$q_i(X,\tau) = \frac{1}{i!}\frac{\partial S^+}{\partial Z^i}(X,0,\tau). \tag{8}$$

$h(X,\tau)$ is an unknown scale factor that is determined by the solution of the integral momentum equation. q_0 and q_1 are related to the unknown temperature and heat flux distributions on the plate wall since $q_0 = S_w^+ = T_w^+ = T_w/T_\infty$ and $q_1 = S_{Zw}^+ = (T/T_{aw})_{Z,0}$ with $T_{aw} = T_\infty(1 + \frac{\gamma-1}{2}M_\infty^2)$, where M_∞ is the free-stream Mach number and T_{aw} is the adiabatic wall temperature in the case of a steady flow over a plate of infinitely small thickness. Finally, the integral formulation of the momentum and energy balance provides the following equations

$$\frac{\partial}{\partial\tau}\left[h\int_0^\infty (1-u^+)\mathrm{d}z\right] + \frac{\partial}{\partial X}\left[h\int_0^\infty u^+(1-u^+)\mathrm{d}z\right] = \frac{1}{h}u_{z,0}^+; \tag{9a}$$

$$\frac{\partial}{\partial\tau}\left[h\int_0^\infty S^+\mathrm{d}z\right] + \frac{\partial}{\partial X}\left[h\int_0^\infty u^+S^+\mathrm{d}z\right] = -\frac{1}{h}S_{z,0}^+. \tag{9b}$$

(We observe that the use of the Taylor's formula instead of a series expansion enables one, by means of a suitable remainder evaluation, to also obtain a good approximation for functions that cannot be expanded in series.)

To complete the model description we need to take into account the energy equation in the solid (3) and formulate the thermal coupling conditions in order to obtain a problem only in terms of unknowns of the fluid field.

4. Coupling of the temperature field between solid and fluid

An integral modelling of the conductive phenomena in the solid plate has been proposed in [4] for $b/L < 1$. In this case the heat Eq. (3), by neglecting terms of order $(\frac{b}{L})^2$, reduces to

$$T_{s,yy} = 0. \tag{10}$$

Eq. (10) admits the solution

$$T_s = T_{sw} + (T_{sw} - T_e)\frac{y}{b}. \tag{11}$$

The Eqs. (10) and (11) and the boundary conditions (6) together with the integral formulation of the heat equation in the solid

$$\frac{1}{\alpha_s}\frac{\partial}{\partial t}\int_{-b}^0 yT_s\,\mathrm{d}y = bT_{sw,y} - T_{sw} + T_e \tag{12}$$

provide the required coupling condition of the temperature field between fluid and solid only in terms of the temperature of the fluid and its derivatives:

$$T_{w,\tau} = 3t_{fs}\left[b\frac{\lambda_\infty}{\lambda_s}T_{w,\eta}(X,\tau) + T_e\right], \tag{13}$$

where $t_{fs} = \frac{L}{U_\infty}\frac{\alpha_s}{b^2}$ is the ratio between the characteristic times of the fluid and of the solid. This relation replaces the boundary conditions (5b) and (6). Therefore we can solve the problem only in the fluid field by solving Eq. (2) with the boundary conditions (4), (5a) and (13).

5. The first-order solution

5.1. Momentum equation

A first order approximation is obtained by using $n = 1$ in Eq. (7a) and adopting $u^+ = Z(z)$ in the integral momentum Eq. (9a) [6,7]. Its integration provides the scale factor of the dynamic boundary layer:

$$H(X,\tau) = h^2(X,\tau) = 4\tau - 8\left(\frac{\tau}{2} - X\right)U_n\left(\frac{\tau}{2} - X\right), \tag{14}$$

with U_n the Heaviside step function.

In the first-order approximation the dynamic boundary layer is characterized by two regions (see Fig. 2) separated by the characteristic line $X = \tau/2$. For $X > \tau/2$ $(h = 2\sqrt{\tau})$ it only depends on time (asymptotic

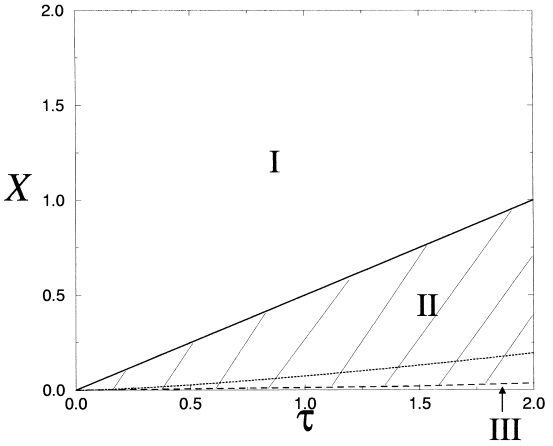

Fig. 2. Characteristic curves in the (X,τ) plane. $M_\infty = 3, p = 1, t_{fs} = 1/3, q_e = -0.25$. I: asymptotic region. II: transition region. III: steady equation region. Continuous line: characteristic curve for the velocity equation. Dotted line: characteristic curve for the energy equation in region I. Dashed line: characteristic curve for the energy equation in region III.

region); it is not influenced by the leading edge and describes a Rayleigh-type flow. For $X < \tau/2$ ($h = \sqrt{8X}$) the velocity field is only depending on X (steady region) and represents a Blasius-type flow.

This solution will be used in the present work. H is continuous in the complete (X,τ) plane while its derivative normal to the characteristic line starting from the origin is discontinuous. However this discontinuity can be eliminated by the higher order approximations. The third order one, for instance, is obtained by using $n = 3$ in Eq. (7a) and adopting $u^+ = Z^3 + g_1(Z - Z^3)$ (for details see Ref. [10]). In this case the derivative of H is continuous and the results (see Fig. 1 of Ref. [10]) are in excellent agreement with the numerical solution proposed in [11].

5.2. Energy equation

A first order approximation of S^+ is similarly obtained by adopting Eq. (7b) with $n = 1$. Then the energy Eq. (9b) and the thermal boundary condition (13) can be written in terms of the unknowns q_0 and q_1 in the following form:

$$2H(d_0 q_{0\tau} + d_1 q_{0X}) + A q_0 = -2\gamma_1 q_1; \tag{15a}$$

$$q_{0\tau}(X,\tau) = 3\gamma_1 \frac{t_{fs} p}{h(X,\tau)} q_1(X,\tau) + 3t_{fs}\left[q_e - q_0(X,\tau)\right]; \tag{15b}$$

with d_0, d_1 and A are constants given by

$$d_0 = \int_0^\infty (1 - Z)\mathrm{d}z = \frac{1}{\pi},\ d_1 = \int_0^\infty Z(1 - Z)\mathrm{d}z = \sqrt{\frac{2}{\pi}} - d_0,\ A = H_\tau d_0 + H_X d_1; \tag{16}$$

while $\gamma_1 = Z'(0) = \frac{2}{\sqrt{\pi}}$, $q_e = \frac{c_p T_e}{H_\infty} - 1$ and $p = \frac{b}{L}\frac{\lambda_\infty}{\lambda_s}\sqrt{Re_\infty}$.

By eliminating q_1 from Eq. (15) we get the first-order hyperbolic equation describing the thermal coupling phenomenon evolution in the (X,τ) plane:

$$\left(d_0 + \frac{1}{3t_{fs} p h}\right) q_{0\tau} + d_1 q_{0X} = \frac{1}{ph}(q_e - q_0) - \frac{A}{2H}. \tag{17}$$

We associate with this first order linear equation two boundary conditions on the X and τ axis. In particular, from the last condition in Eq. (4) we have $T(X,0,0) = T_\infty$ and therefore at the interface $q_0(X,0) = S_w^+(X) = -(\gamma - 1)M_\infty^2/[2 + (\gamma - 1)M_\infty^2]$ with γ the ratio between the specific heats. By denoting this quantity with $q_{0\infty}$ the condition on the X-axis results in

$$q_0(X,0) = q_{0\infty}. \tag{18}$$

The boundary condition on the τ-axis follows from Eq. (6), i.e. from the continuity of the temperature and heat flux at the interface applied for $X = 0$. The heat flux in the solid body is given by $(T_w - T_e)/b$ and therefore is a finite quantity; on the other side it is proportional to $q_1/h(X)$ and hence, because $h(0) = 0$, it follows $q_1(0,\tau) = 0$. Moreover, assuming $T(0,\tau)$ finite and from Eq. (15a) (the energy equation in the fluid evaluated at $X = 0$, with $h(0) = 0$) we have

$$q_0(0,\tau) = 0, \tag{19}$$

which is the required boundary condition on τ. We note that this condition leads to $T_w(0,\tau) = T_{aw}$.

The Eq. (17) can be analytically solved by using the Lagrange's method (see Appendix A). For the energy field three main regions have been found.

5.2.1. $X > \tau/2$, asymptotic region

$$q_0(X,\tau) = q_{0\infty} q_{0a}(\tau) + q_{0p}(\tau), \tag{20}$$

with

$$q_0 a(\tau) = \left(6d_0 t_{fs} p^2 \sqrt{\frac{\tau}{p^2}} + 1\right)^{-a} \exp\left(\frac{-1}{d_0}\sqrt{\frac{\tau}{p^2}}\right);$$

$$q_{0p}(\tau) = q_e q_{0a}(\tau) 3t_{fs} p^2 \int_0^{\frac{\tau}{p^2}} \left(6t_{fs} p^2 d_0 \sqrt{\frac{\bar{\tau}}{p^2}} + 1\right)^{(a-1)} \exp\left(\frac{1}{d_0}\sqrt{\frac{\bar{\tau}}{p^2}}\right)\frac{d\bar{\tau}}{p^2}; \tag{21}$$

where $a = 1 - 1/(6t_{fs} p^2 d_0^2)$. This solution can also be directly obtained by solving the first-order ordinary equation obtained by neglecting the spatial derivative in Eq. (17). The region has been denoted by I in Fig. 2.

5.2.2. Steady region

This region (III in Fig. 2) is identified by $\tau > \phi(X)$, where the curve $\tau = \phi(X)$ is the characteristic curve of the energy equation

$$\tau = \frac{d_0}{d_1} X + \frac{1}{3\sqrt{2} t_{fs} p}\sqrt{X} = \phi(X). \tag{22}$$

The solution is here

$$q_0(X,\tau) = Q_0(\xi) = q_e\left\{1 - \frac{1}{\xi}\left[1 - \exp(-\xi)\right]\right\};$$

$$\xi = \frac{1}{\sqrt{2} d_1}\sqrt{\frac{X}{p^2}}. \tag{23}$$

Similarly to the asymptotic region, this integral can be directly obtained by solving Eq. (17) with $q_{0\tau} = 0$.

5.2.3. $\tau < \phi(X)$, transition region

The solution (II in Fig. 2) is given by the equation

$$\frac{q_0(X,\tau) - Q_0(X)}{Q_{0a}(X)} = F\big[\tau - \phi(X)\big], \tag{24}$$

with

$$Q_{0a}(X) = \left(\frac{X}{p^2}\right)^{-1/2} \exp\left(-\frac{1}{\sqrt{2}d_1}\sqrt{\frac{X}{p^2}}\right). \tag{25}$$

The function $F[\tau - \phi(x)]$ is given by

$$F\big[\tau - \phi(X)\big] = F(s) = \frac{q_0\big[\psi(s)/2,\psi(s)\big] - Q_0\big[\psi(s)/2\big]}{Q_{0a}\big[\psi(s)/2\big]}, \tag{26}$$

with

$$\psi(s) = \left(\frac{k_1 + \sqrt{k_1^2 + 2k_2 s}}{k_2}\right)^2;$$

$$k_1 = \frac{1}{6t_{\mathrm{fs}}pd_1};\ k_2 = \frac{2d_1 - d_0}{d_1}. \tag{27}$$

In Figs. 3 and 4 the present solution is compared to the 'exact' ones [4,9] and to the preliminary lower order results [5] obtained in the asymptotic and steady regions for the energy. The temperature on the wall is directly connected to q_0 and is given by

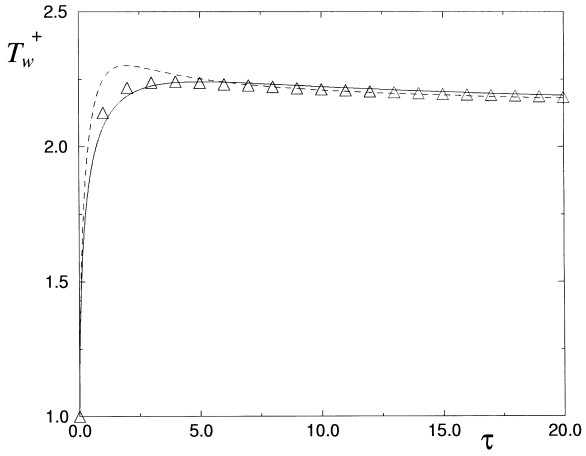

Fig. 3. T_w^+ versus τ in the asymptotic region. $M_\infty = 3$, $p = 1$, $t_{\mathrm{fs}} = 1/3$, $q_{\mathrm{e}} = -0.25$. Symbols: 'exact' solution; continuous line: present solution; dashed line: 0-order solution.

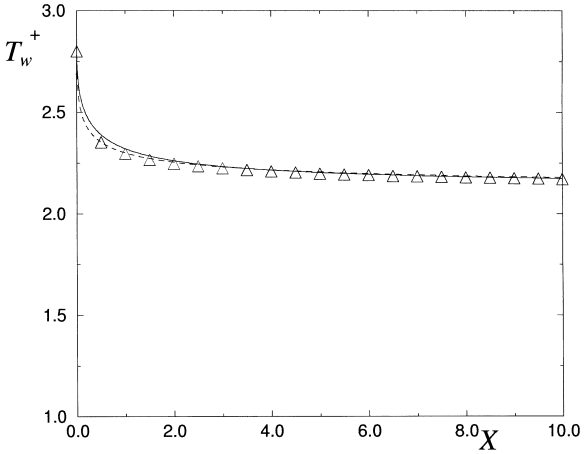

Fig. 4. T_w^+ versus X in the steady region. $M_\infty = 3$, $p = 1$, $t_{\mathrm{fs}} = 1/3$, $q_{\mathrm{e}} = -0.25$. Symbols: 'exact' solution; continuous line: present solution; dashed line: 0-order solution.

$$T_w^+ = (q_0 + 1)\left(1 + \frac{\gamma - 1}{2}M_\infty^2\right). \tag{28}$$

The results are good, the improved accuracy of the first-order solution is shown especially in the asymptotic region and in the steady region for larger values of X.

As anticipated in the introduction the main progress of the present work is given by the determination of a solution in the complete plane (X,τ) that, on the contrary of [5] exactly satisfies an integral formulation of the energy equation and not only the coupling condition (15b). In Fig. 5 an example is shown; the temperature on the plate is plotted versus X for different values of time.

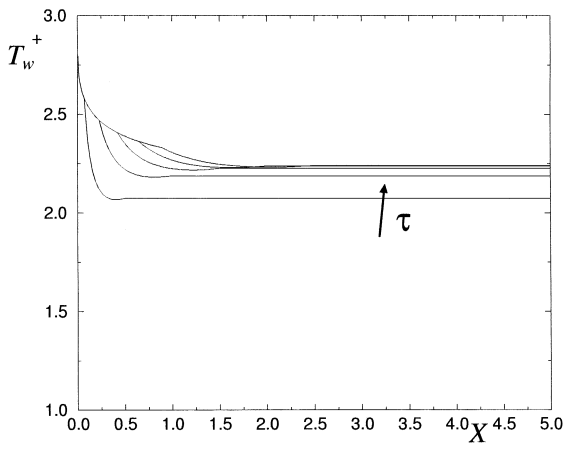

Fig. 5. T_w^+ versus X. $\tau = 1, 2, 3, 4, 5$. $M_\infty = 3$, $p = 1$, $t_{\mathrm{fs}} = 1/3$, $q_{\mathrm{e}} = -0.25$.

6. The local solution in the origin

It is very interesting to analyse the behaviour of the solution in the neighbourood of the origin of the (X,τ) plane since the solution is singular in (0, 0). In fact from the asymptotic solution it is

$$\lim_{X,\tau\to 0} q_0(X,\tau) = q_{0\infty}, \tag{29}$$

while in the steady region we have

$$\lim_{X,\tau\to 0} q_0(X,\tau) = \lim_{X\to 0} Q_0(X) = 0. \tag{30}$$

For small values of τ the solution in the asymptotic region can be further simplified if the terms greater than $O(\tau)$ are neglected thus obtaining

$$q_0(\tau) = q_{0a}(\tau)(q_{0\infty} + q_e q_{0l}(\tau)),$$

$$q_{0l}(\tau) = 6t_{fs}p^2 d_0^2 \left[\exp\left(\frac{1}{d_0}\sqrt{\frac{\tau}{p^2}}\right) \left(\frac{3}{d_0}\sqrt{\frac{\tau}{p^2}} - \frac{1}{d_0^2}\frac{\tau}{p^2} - 3\right) + 3 \right]. \tag{31}$$

In a similar way, neglecting terms greater than $O(\xi)$, the solution in the steady region is approximated by

$$q_0(X) = \frac{1}{2\sqrt{2}d_1}\sqrt{\frac{X}{p^2}}. \tag{32}$$

The local solution is compared to the complete one in Fig. 6 showing the good accuracy for small values of X and τ.

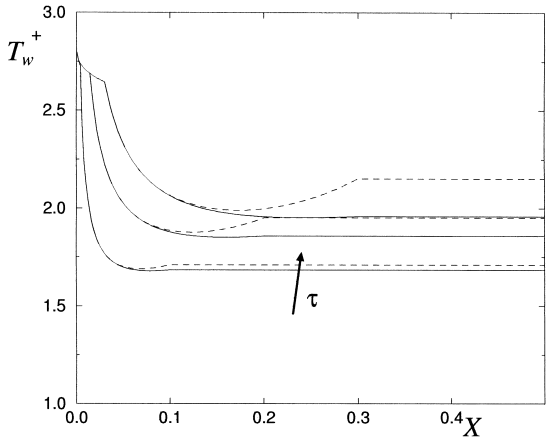

Fig. 6. T_w^+ versus X; comparison between local and global solution. $M_\infty = 3$, $p = 1$, $t_{fs} = 1/3$, $q_e = -0.25$. Continuous line: complete solution; dashed line: local solution. $\tau = 0.2$, 0.4, 0.6.

7. Analysis of the results

Together with the M_∞ two non-dimensional groups completely characterize the phenomenon. They are p (related to the geometry, the ratio of the thermal conductivities and the Reynolds number) and t_{fs} which is the ratio between the characteristic times of the fluid and of the solid.

The heat flux at the solid–fluid interface is given by

$$J_{qw} = -\lambda_{fw} T_{w,y} = -\lambda_\infty \frac{\gamma_1 T_{Z,0}\sqrt{Re_\infty}}{Lh} \tag{33}$$

and it is directly connected with q_1 since $T_{Z,0} = S^+_{Z,0} T_{aw} = q_1 T_{aw}$.

7.1. Asymptotic region

It is interesting to note that the solution only depends on the independent variable τ/p^2, on the parameters q_e and on

$$\delta = 3t_{fs}p^2 = 3\frac{1}{Pr}\frac{\lambda_\infty}{\lambda_s}\frac{\rho_\infty}{\rho_s}\frac{c_{pf}}{c_s}, \tag{34}$$

where c_{pf} and c_s are respectively the specific heat of the fluid at constant pressure and the specific heat of the solid. In Fig. 7, T_w/T_{aw} is plotted versus τ/p^2 for different values of δ and a specified q_e. The peak temperature value only depends on δ and not on the plate thickness while the asymptotic temperature is T_e. The plate thickness (present in the parameter p but not in δ) only affects the times at which the peak and the asymptotic values are reached. $(T/T_{aw})_{Z,0}$ at the solid–fluid interface is plotted in Fig. 8 for the same values of δ and q_e. It is finite for $\tau/p^2 = 0$ and again the minimum value only depends on δ and q_e. The limiting behaviours of the wall temperature for $\tau\to 0^+$ and $\tau\to\infty$ are:

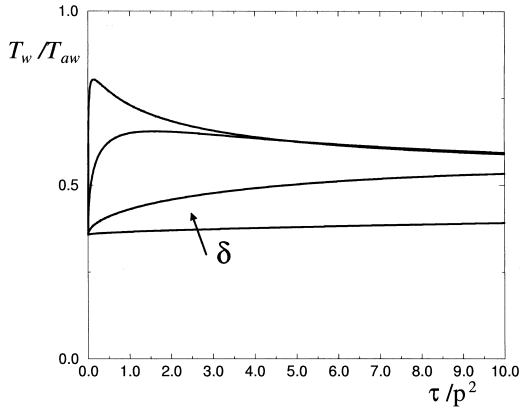

Fig. 7. T_w/T_{aw} versus τ/p^2. $\delta = 0.01$, 0.1, 1, 10.

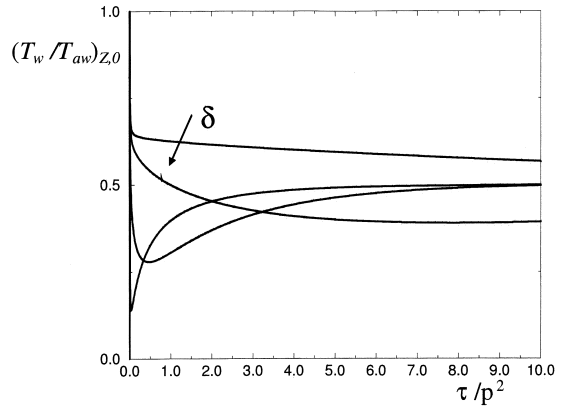

Fig. 8. $(T/T_{\mathrm{aw}})_{Z,0}$ versus τ/p^2. $\delta = 0.01, 0.1, 1, 10$.

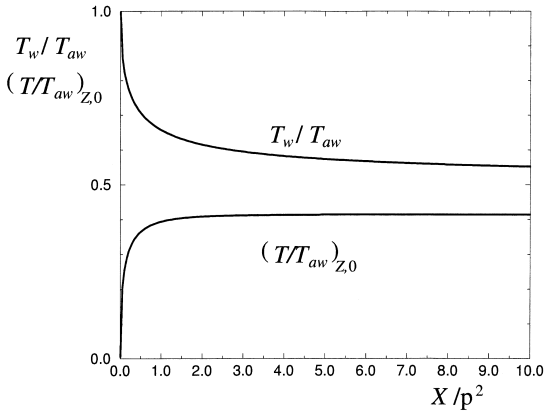

Fig. 9. T_w/T_{aw} and $(T/T_{\mathrm{aw}})_{Z,0}$ versus X/p^2.

$$\tau\to 0^+:\frac{T_w}{T_{\mathrm{aw}}}\to 1+q_{0\infty}\left(1-2\delta d_0\sqrt{\frac{\tau}{p^2}}\right),$$

$$\tau\to\infty:\frac{T_w}{T_{\mathrm{aw}}}\to\frac{T_{\mathrm{e}}}{T_{\mathrm{aw}}}+\frac{\sqrt{2}d_0}{\sqrt{\frac{\tau}{p^2}}}\left(1-\frac{T_{\mathrm{e}}}{T_{\mathrm{aw}}}\right); \tag{35}$$

while the heat fluxes are:

$$\tau\to 0^+:\left(\frac{T_w}{T_{\mathrm{aw}}}\right)_{Z,0}\to -q_{0\infty}\left(1-\frac{4}{\sqrt{\pi}}\delta\sqrt{\frac{\tau}{p^2}}\right),$$

$$\tau\to\infty:\left(\frac{T_w}{T_{\mathrm{aw}}}\right)_{Z,0}\to -q_{\mathrm{e}}. \tag{36}$$

These behaviours are in perfect agreement with the exact solution [4]. In particular, we recover the result that, for very small values of time, the solution is independent of the temperature T_{e} imposed on the unwetted plate side (the influence of T_{e} appears with the terms $O(\tau/p^2)$). We note that, while the temperature is continuous, for $\tau = 0$ the heat flux $T_{Z,0}/h$ is infinite. The asymptotic behaviour $(\tau/p^2\to\infty)$ also describes the solution in the case of a plate of infinitely small thickness ($b = 0$). In this case the temperature and the heat flux on the wall impulsively assume the asymptotic constant values.

7.2. Steady region for the energy equation

In this region (identified with III in Fig. 2) the solution only depends on the independent variable X/p^2 and on the parameter q_{e}. Again p does not influence the values of the temperature at heat flux at the wall but only the spatial coordinate at which the values are obtained. In Fig. 9, T_w/T_{aw} and $(T/T_{\mathrm{aw}})_{Z,0}$ are plotted against X/p^2.

The limiting behaviours of the temperature are the following:

$$X\to 0^+:\frac{T_w}{T_{\mathrm{aw}}}\to 1+q_{\mathrm{e}}\frac{\sqrt{2}}{4d_1}\sqrt{\frac{X}{p^2}},$$

$$X\to\infty:\frac{T_w}{T_{\mathrm{aw}}}\to 1+q_{\mathrm{e}}\left(1-\frac{\sqrt{2}d_1}{\sqrt{\frac{X}{p^2}}}\right); \tag{37}$$

while for the heat flux:

$$X\to 0^+:\left(\frac{T_{\mathrm{w}}}{T_{\mathrm{aw}}}\right)_{Z,0}\to -q_{\mathrm{e}}2\sqrt{2}\sqrt{\frac{X}{p^2}}, \tag{38a}$$

$$X\to\infty:\left(\frac{T_{\mathrm{w}}}{T_{\mathrm{aw}}}\right)_{Z,0}\to -4\frac{d_1}{\gamma_1}q_{\mathrm{e}}. \tag{38b}$$

Due to the boundary condition (19) we have $T_w = T_{\mathrm{aw}}$ at the plate leading edge while for $X\to\infty$ is: $T_w\to T_{\mathrm{e}}$. The heat flux $T_{Z,0}/h$ is finite at the leading edge while tends to 0 with the law $1/h$ for large values of X.

It is interesting to compare present results to the limiting solution relative to a steady flow over a flat plate of infinitely small thickness ($b = 0, T_w = T_{\mathrm{e}}$):

$$S^+(X,z) = q_{\mathrm{e}}(1-u^+), \tag{39a}$$

$$S^+_{Z,0} = \left(\frac{T_{\mathrm{w}}}{T_{\mathrm{aw}}}\right)_{Z,0} = -4\frac{d_1}{\gamma_1}q_{\mathrm{e}}. \tag{39b}$$

For $X\to\infty$ this solution is equal to the Eq. (38b); on the contrary the finite thickness of plate strongly modifies the solution near the leading edge. In particular, the heat flux reduces from an infinite value to a finite one at the plate apex:

$$\frac{T_{wZ,0}}{(T_{wZ,0})_{ref}} = 1 - \exp\left(\frac{1}{\sqrt{2}d_1}\sqrt{\frac{X}{p^2}}\right), \tag{40}$$

where $(T_{Z,0})_{ref}$ is given by Eq. (39b).

7.3. Temperature and velocity profiles

We present here some results for a practical problem in which a metal plate characterized by $b/L = 0.01$ is accelerated in a high-speed air flow. The value of T_e is lower than the adiabatic temperature (for steady flow) so the fluid is heating the plate.

Due to the small value of t_{fs} a sufficient extension of the steady region for the energy equation is only reached for large values of τ.

The integral boundary layer equations have been obtained by a first order description of the velocity and temperature profiles ($n = 1$ in Eq. (7b)). However, more accurate profiles can be derived since the coefficients q_i for $i > 1$ can be determined in terms of (q_0,q_1) by using the energy Eq. (2c) evaluated at the wall. In particular, we also computed q_2 by the relation

$$q_2 = \frac{H(X,\tau)}{2\gamma_1^2} q_{0\tau}(X,\tau), \tag{41}$$

obtaining a third-order description of the temperature profiles:

$$S^+(X,Z,\tau) = q_0(X,\tau)(1 - Z^3) + q_1(X,\tau)(Z - Z^3) + q_2(X,\tau)(Z^2 - Z^3),$$

$$T^+(X,Z,\tau) = \frac{T_{aw}}{T_\infty}\left[1 + S^+(X,Z,\tau)\right] - \frac{\gamma - 1}{2} M_\infty^2 Z^2 \tag{42}$$

Some temperature distributions in the fluid for different Mach numbers are shown in Fig. 10. In this example the solution is still in the transition region. Fig. 11 shows the difference between the temperature profiles when plotted against the physical and the Stewartson–Dorodnitsin normal coordinate to the wall. Finally by present solution it is possible to show the time evolution of the thermal (Fig. 12) and of the velocity (Fig. 13) fields. The values $\tau = 10$, 1000, 10,000 characterize respectively an early transition, transition and steady region for the energy.

8. Conclusions

We have here presented an analysis of the thermo-

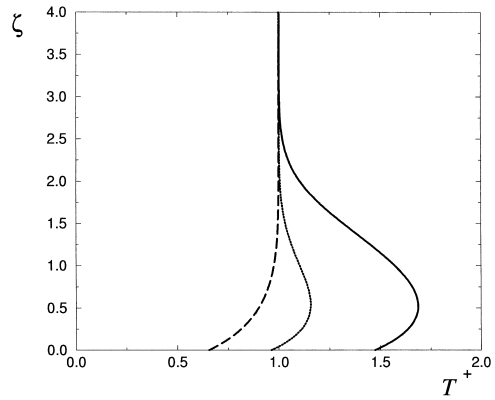

Fig. 10. T^+ versus $\zeta = \frac{y\sqrt{Re_\infty}}{Lh}$. $p = 0.0329$, $t_{fs} = 0.000933$, $q_e = -0.522$, $X = 0.01$, $\tau = 1000$. Continuous line: $M_\infty = 3$; dotted line: $M_\infty = 2$; dashed line: $M_\infty = 1$.

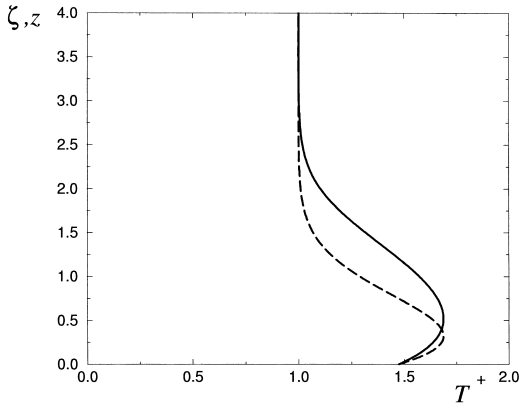

Fig. 11. T^+ versus $\zeta = \frac{y\sqrt{Re_\infty}}{Lh}$ (continuous line) and z (dashed line). $M_\infty = 3$, $p = 0.0329$, $t_{fs} = 0.000933$, $q_e = -0.522$, $p = 0.0329$, $t_{fs} = 0.000933$, $q_e = -0.522$, $X = 0.01$, $\tau = 1000$.

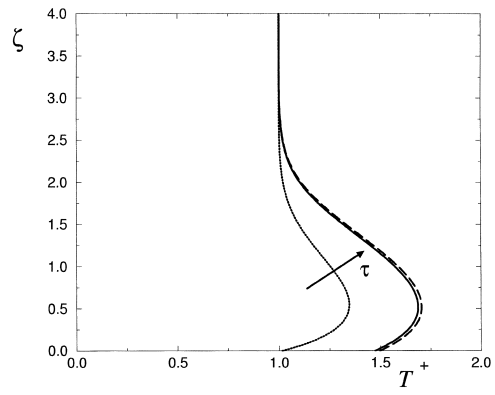

Fig. 12. T^+ versus $\zeta = \frac{y\sqrt{Re_\infty}}{Lh}$. $M_\infty = 3$, $p = 0.0329$, $t_{fs} = 0.000933$, $q_e = -0.522$, $X = 0.01$. Dotted line: $\tau = 10$; continuous line: $\tau = 1000$; dashed line: $\tau = 10{,}000$.

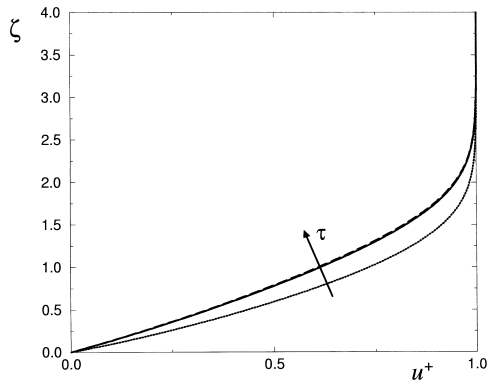

Fig. 13. u^+ versus $\zeta = \frac{y\sqrt{Re_\infty}}{Lh}$. $M\infty = 3$, $p = 0.0329$, $t_{fs} = 0.000933$, $q_e = -0.522$, $X = 0.01$. Dotted line: $\tau = 10$; continuous line: $\tau = 1000$; dashed line: $\tau = 10{,}000$.

fluid dynamic field arising above a semi-infinite flat plate that is impulsively accelerated in a compressible laminar flow taking also into account the effect of the finite thickness of the solid plate and of its thermal conductivity. We used an integral formulation for the boundary layer and for the solid–fluid thermal coupling. The equations have been integrated in a quasi-analytical form by the Lagrange's method.

There are many reasons making this study useful. Despite of the simplicity of the geometry this problem is still complex as also demonstrated by the lack of results in literature. A first difficulty arises from the three-dimensional nature of the problem (the variables are x, y, t). Moreover, the problem is complicated by the presence of the singularity in the origin of the plane (X,τ). This singularity does not enable to easily find a numerical solution (for example, by the method of the characteristic) because the usual interpolations formulae are critical to apply near the singularity.

Present analytical results allowed to understand the main features of the phenomenon. Three regions have been identified: they are characterized by strong different behaviours. In particular, there is an asymptotic region for the velocity and energy field in which the flow is depending only on time, it is of Rayleigh-type and not influenced by the plate leading edge. For large values of time (or equivalently very near the leading edge) the solution is depending only on X. Finally a transition region for the energy is present, in which the flow depends both on time and space.

The results have been compared to 'exact' solutions that hold for the limiting conditions of asymptotic flow (no leading edge influence) and steady flow showing good accuracy.

The non-dimensional parameters governing the regimes have been determined and their influence is easily shown by the simple analytical relations.

Finally the presence of a singularity of the solution in the origin of the (X,τ) plane makes this reference solution meaningful to attempt for a numerical solution of the problem in more complex geometries.

Acknowledgements

This work was supported by MURST (Italian Ministry of University and Research)

Appendix. The Lagrange's method

Given the quasi linear first order equation

$$a_1 q_x(x,t) + a_2 q_t(x,t) = a_3 \tag{A1}$$

where $a_i = a_i(x,t,q)$, we obtain a well defined problem if $q[x_c(s),t_c(s)] = \bar{q}(s)$ is known on a non-characteristic curve c defined by the parametric equations $x_c(s)$, $t_c(s)$. It is possible to derive the solution of this problem in its existence domain by applying the Lagrange's method. It consists in determining two independent solutions, in the form

$$f(x,t,q) = c_1, \quad g(x,t,q) = c_2, \tag{A2}$$

of the characteristic system

$$\frac{dx}{a_1} = \frac{dt}{a_2} = \frac{dq}{a_3}. \tag{A3}$$

Finally the general solution of the Eq. (A1) can be written in the form $g = G(f)$ or $f = F(g)$ where the function G or F can be determined by imposing the boundary condition on the curve c.

For the Eq. (17) we have $q = q_0, a_1 = d_1, a_2 = d_0 + 1/(3t_{fs}ph), a_3 = (q_e - q_0)/(ph) - A/(2H)$ and, obviously, $x = X$, $t = \tau$.

In the asymptotic region $(X > \tau/2, h = h(\tau))$ we solve the characteristic system

$$\frac{dX}{d\tau} = \frac{a_1}{a_2}, \quad \frac{dq_0}{d\tau} = \frac{a_3}{a_2}. \tag{A4}$$

The solution of the first equation $(f(X,\tau,q_0) = c_1)$ provides the family of the characteristic curves:

$$X - \frac{d_1}{d_0}\tau + \frac{1}{3t_{fs}p} d_1 d_0^2 \sqrt{\tau} - \frac{d_1}{2(3t_{fs}p)^2 d_0^3} \log\left(\frac{2\sqrt{\tau} + \frac{1}{3t_{fs}pd_0}}{\frac{1}{3t_{fs}pd_0}} \right) = X - \sigma(\tau) = c_1, \tag{A5}$$

while from the second one we obtain $g(X,\tau,q_0)$:

$$\frac{q_0 - q_{0p}}{q_{0a}} = c_2 \tag{A6}$$

where q_{0p} and q_{0a} are given by relations (21).

Hence the general solution of Eq. (17) in the asymptotic region is:

$$\frac{q_0 - q_{0p}}{q_{0a}} = F\big[X - \sigma(\tau)\big]. \tag{A7}$$

The function F is determined by imposing the boundary condition $q_0(X,0) = q_{0\infty}$ obtaining

$$F\big[X - \sigma(\tau)\big] = \text{const} = q_{0\infty} \tag{A8}$$

and the relation (20) is recovered. For $X < \tau/2$, the characteristic system is:

$$\frac{\mathrm{d}X}{\mathrm{d}\tau} = \frac{a_1}{a_2}, \quad \frac{\mathrm{d}q_0}{\mathrm{d}\tau} = \frac{a_3}{a_1}. \tag{A9}$$

Following the same steps of the previous case $f(X,\tau,q_0)$ is:

$$\tau - \phi(X) = c_1, \tag{A10}$$

where $\phi(X)$ is given by Eq. (22).

$g(X,\tau,q_0)$ is given by

$$\frac{q_0 - Q_0}{Q_{0a}} = c_2, \tag{A11}$$

where Q_0 and Q_{0a} are given in Eqs. (23) and (25).The general integral can be written as

$$\frac{q_0 - Q_0}{Q_{0a}} = F\big[\tau - \phi(X)\big] = f_1(s) + f_2(s). \tag{A12}$$

$f_1(s)$ is again obtained by imposing the boundary condition $(q_0(0,\tau) = 0)$ and is $f_1(s) = 0$. $f_2(s) = F(s)$ is determined by imposing the continuity of q_0 across the line $X = \tau/2$ and it is given by relations (26) and (27).

References

[1] A.V. Luikov, V.A. Aleksashenko, A.A. Aleksashenko, Analytical methods of solution of conjugated problems in convective heat transfer, Int. J. Heat Mass Transfer 14 (1971) 1047–1056.

[2] S. Mori, M. Sakaribara, A. Tanimoto, Steady heat transfer to laminar flow in a circular tube with conduction in the tube wall, Heat Transfer Jap. Res 3 (2) (1974) 37–46.

[3] S. Mori, T. Shinke, M. Sakaribara, Steady heat transfer to laminar flow between parallel plates with conduction in wall, Heat Transfer Jap. Res 5 (4) (1976) 17–25.

[4] A. Pozzi, E. Bassano, L. de Socio, Coupling of conduction and forced convection past an impulsively started infinite flat plate, Int. J. Heat Mass Transfer 36 (7) (1993) 1799–1806.

[5] A Pozzi, E Bassano, Coupling of conduction and convection past an impulsively started semi-infinite flat plate for Prandtl number equal to one, in: Proceedings of XI Congresso Nazionale AIMETA. Trento, Italy, 1992, pp. 127–132.

[6] A. Pozzi, A.R. Teodori, Separation points in laminar flow, Meccanica 28 (1993) 53–59.

[7] A. Pozzi, L. Mazzei, An integral method for compressible laminar boundary layer, J. Heat Transfer 120 (1998) 505–506.

[8] A Pozzi, R Tognaccini, Coupling of conduction and convection past an impulsively started semi-infinite flat plate for Prandtl number equal to one (part II), in: Third European Symposium on Aerothermodynamics for Space Vehicles, Noordwijk, NL, SP-426, 1999, pp. 317–324.

[9] A. Pozzi, M. Lupo, The coupling of conduction with forced convection over a flat plate, Int. J. Heat Mass Transfer 32 (7) (1989) 1207–1214.

[10] P.G. Berardi, A. Pozzi, Unsteady momentum and energy boundary layers in laminar flat plate flow, Int. J. Heat Mass Transfer 28 (1) (1985) 101–109.

[11] C.B. Watkins, Unsteady heat transfer in impulsive Falkner–Skan flows. Int. J. Heat Mass Transfer 19(1) (1976) 395–403.